The influence of the cloud cover on aridity over the Mongolian Plateau from 1979~2019

Jie He (1), Enliang Guo (2), Shanhu Bao (2), Husi Letu (1)

[1] Aerospace Information Research Institute, Chinese Academy of Sciences, 20 Datun road, Chaoyang District, Beijing, 100101, China
[2] College of Geography Science, Inner Mongolia Normal University, Hohhot, 010010, China
Email: hejie@aircas.ac.cn;

KEY WORDS: Total precipitation; Potential evaporation; Surface radiation; Low cloud cover

ABSTRACT: Cloud cover can affect aridity by affecting precipitation and surface radiation. However, a comprehensive study the effects of cloud cover, energy and water cycle parameters on aridity are lacking over the Mongolian Plateau (MP). In this study, the spatiotemporal variation characteristics of cloud cover and aridity index are analyzed, and the causes of aridity are found out from the influence of cloud cover on energy and water cycle parameters by European Centre for Medium Range Weather Forecasting (ECMWF) ERA5 reanalysis dataset from 1979~2019. The research parameters include low cloud cover, medium cloud cover, high cloud cover and total cloud cover. Potential evaporation and total precipitation are used to calculate the aridity index. Correlation coefficients is used to analyze the relationship between the aridity index and research parameters. Spatiotemporal variation characteristics is used to analyze the cause of aridity. Cloud cover was used to analyze the interaction between energy and water cycle parameters. The results indicate that cloud cover is only 40 % and keep fall especially since 1999. Aridity index has been above an average of 40 % for 13 of the 21 years from 1999~2019. Less cloud cover leads the total precipitation less than 400 mm. The low cloud cover causes the increase of surface radiation from 1979~2019, especially the surface net longwave radiation. It leads to an increase in potential evaporation (>800 mm), which is twice as much as total precipitation in arid regions. A comprehensive study shows that low cloud cover is the main cause of aridity over MP. The analysis and prediction of the cloud cover parameters are helpful for aridity disaster prevention and early warning.

1. Introduction

The Mongolian plateau (MP) is an arid and semi-arid plateau, and its aridity conditions are increasingly serious and have an impact on the surrounding areas. Cloud cover affects aridity through the following parameters such as surface radiation, precipitation, evapotranspiration, all these parameters together affect the aridity over the MP and its surrounding areas. However, the current studies on aridity over the MP and its surrounding areas are lack of research on the effects of cloud cover on aridity. A comprehensive study on the distribution of cloud cover, energy and water cycle parameters is helpful to find out the cause of aridity.

The current aridity research usually take a few key parameters, such as the circulation index, vegetation, temperature, desertification, precipitation and evapotranspiration over the MP and its surrounding areas (Jin et al., 2019; Li et al., 2018; Dyn et al., 2014; Hessl et al., 2018; Tong et al., 2018). Studies show that atmospheric circulation can affect drought over the MP because the weakening of the subtropical high in the western Pacific and the increase in the East Asian Arctic vortex negatively impact spring precipitation transport (Gao et al., 2019). There is a linear relationship between surface net shortwave radiation and surface temperature, and such a relationship is significantly correlated with soil moisture, which will help to predict drought (Song et al., 2012). Pedram proved that soil moisture on no rainfall days is related to soil temperature, while that on rainy days is related to atmospheric precipitation (Pedram et al., 2017; Cao et al., 2017). Other studies have examined the effects of latent heat and evapotranspiration on aridity. Some studies have shown that aridity leads to a decrease in vegetation cover, which further leads to a decrease in seasonal latent heat and surface temperature (Bremer et al., 2001). Some studies focus on temperature and precipitation. The study shows that with the increase in precipitation and temperature, the vegetation cover in the former MP continued to increase in the mid-1990s but decreased after 1990 when precipitation decreased. With increasing temperature, the negative correlation of precipitation with aridity will increase (Hu et al., 2018).

The most important drought research method is the drought index, which includes the Palmer drought severity index (PDSI), standardized precipitation index (SPI), standardized precipitation evapotranspiration index (SPEI) and aridity index. The PDSI is calculated by evapotranspiration, precipitation, and soil moisture (Alley, 1984). The SPI is calculated by precipitation (McKee et al., 1993). The SPEI is a normalized calculation of precipitation and potential evapotranspiration difference (Vicente-Serrano et al., 2010). The aridity index is used in this paper, which is calculated by potential evaporation and precipitation. The aridity index formula has the advantage that potential evaporation is based on energy balance, water vapor pressure and temperature parameters, and this formula has a solid theoretical basis and physical significance (Penman, 1948). The above drought indexes have been applied over the MP. For example, Studies show that PDSI began to drop from 4 to -2 in 1960~2010 over the MP (Hessl et al., 2018). The drought was most severe in spring over the MP from 1980~2015 (Jin et al., 2019). As a result of the surrounding climate forcing, droughts began to get worse (SPEI<−4.307) after 1999 over the MP (Dyn et al., 2014). 72.2 % of the MP is arid from 1980~2014, and the SPEI fell by -0.0113 per year (Tong et al., 2018). At present, drought research methods include correlation analysis, principal component analysis and the Mann-Kendall test, which are used to analyze the influence of parameters on the drought index and change trend.

There is a lack of comprehensive cloud cover, energy and water cycle parameters to study aridity over the MP and surrounding areas. The innovation of this paper is to comprehensive study the influence of Cloud cover at different heights, total precipitation, potential evaporation, surface radiation on aridity over the MP and surrounding areas. The comparison of precipitation and evaporation determines the degree of aridity; The surface radiation is the power of evaporation, while evaporation also affects cloud formation; Cloud cover is the key parameter for precipitation and cloud affect surface radiation through cloud radiative forcing (Penman, 1948; Katata et al., 2008; Bao et al., 2020). The effects of the above parameters on aridity are complex. Therefore, random forest method is adopted in this paper to find the most important parameters. European Centre for Medium Range Weather Forecasts (ECMWF) ERA5 reanalysis dataset is used in this paper. There are several types of reanalysis dataset available, for example, the ECMWF/ERA15, ERA-INTERIM and the latest ERA5 (Bauer et al., 2007; Balsamo et al., 2015); the National Center for Environmental Prediction, National Center for Atmospheric Research (NCEP/NCAR) reanalysis dataset (Betts et al., 1996) and the NASA Goddard Earth Observing System (GEOS) reanalysis dataset (Young et al., 2012; Molod et al., 2017). The latest ERA5 reanalysis dataset has long time series and higher spatial and temporal resolution (0.25°, 1 h) (Urraca et al., 2018), which is more suitable for aridity research over the MP.

We first studied the correlation of cloud cover to the aridity index over the MP and surrounding areas. Then the spatiotemporal variation characteristics of cloud cover and aridity index are analyzed. The influence of cloud cover on energy and water cycle key parameters are analyzed to find out the causes of aridity. The paper is organized as follows. Section 2 describe the study area, datasets and methods. Section 3 presents the relationship between the research parameters and the aridity index. The characteristics of the spatial and temporal distribution of the cloud cover and aridity index. The causes of aridity were analyzed from the spatial and temporal distribution of energy and water cycle key parameters. Finally, we present our conclusions in Section 4.

2. Data and methods

2.1 Research area

The research area in this paper is rectangular, covering the whole MP and some surrounding areas, including the whole of Mongolia and part of China and Russia. As shown in Figure 1 (a), the latitude range is 37°N to 53.5°N, and the longitude range is 87.5°E to 126°E. Composed mainly of mountains and high-altitude plains, the MP is a complex terrain with an average elevation of 1,580 meters.

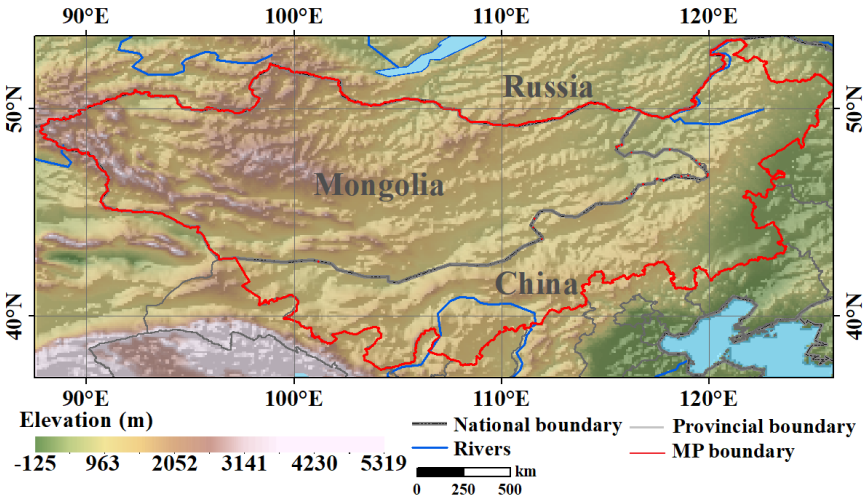

Fig. 1 DEM of the study area

2.2 Data

ERA5 is the global climate reanalysis dataset that were released on 17 July 2017 by the Copernican climate change service operated by the ECMWF, which mainly includes atmospheric parameters and surface parameter data (Bauer et al., 2007; Balsamo et al., 2015). ERA5 reanalysis dataset are produced by using the existing observation data assimilation method. These data have the characteristics of global coverage, long time series and high spatial and temporal resolution and can be used in the study of climate and weather forecasts (Bengtsson et al., 2004). The ERA5 reanalysis dataset used in this paper are 'ERA5 monthly averaged data on single levels from 1979 to present'. The spatial and temporal resolutions of this dataset are 0.25° and monthly.

The cloud cover parameters include Low cloud cover (LCC), Medium cloud cover (MCC), High cloud cover (HCC) and Total cloud cover (TCC). The energy and water cycle key parameters we use include Surface net shortwave radiation (SNSR), Surface net longwave radiation (SNLR), Surface total radiation (R_n), Total precipitation (TP), Potential evaporation (PE).

2.3 Methods

The aridity index (AI) is normally defined as AI=PE/TP (Wu et al., 2006; Weerts et al., 2013). The AI not only involves key parameters of the water cycle but also potential evaporation related to energy cycle parameters, air temperature, soil heat flux density, slope vapor pressure curve, slope vapor pressure curve, radiation and wind speed (Penman, 1948). We calculated the annual mean AI and determined the aridity conditions of the region according to the value range: humid ($AI < 1.00$), subhumid ($1.00 \leq AI < 1.50$), semiarid ($1.50 \leq AI < 4.00$) and arid ($AI \geq 4.00$) (Wu et al., 2006).

To study the variation trend of aridity, energy and water cycle parameters, the Mann-Kendall method is used in this paper (Mann, 1945; Kendall, 1990). As shown in Formula 1, to calculate the standardized Mann-Kendall statistic Z_S, we first calculate the test statistic S defined as Formula 2, where x_j and x_i are the sequential data values, and n is the length of the data. As shown in Formula 4, Mann-Kendall proved that when n>8, the statistic S is approximately normally distributed with the mean and variance. $V(S)$ is the variance, where t_i is the number of ties of extent i.

$$Z_S = \begin{cases} \dfrac{S-1}{\sqrt{V(S)}}, & S > 0 \\ 0, & S = 0 \\ \dfrac{S+1}{\sqrt{V(S)}}, & S < 0 \end{cases} \quad (1)$$

Where S is

$$S = \sum_{i=1}^{n-1} \sum_{j=i+1}^{n} \mathrm{sgn}(x_j - x_i) \quad (2)$$

$$\mathrm{sgn}(x_j - x_i) = \begin{cases} +1, & (x_j - x_i) > 0 \\ 0, & (x_j - x_i) = 0 \\ -1, & (x_j - x_i) < 0 \end{cases} \quad (3)$$

$$V(S) = \frac{n(n-1)(2n+5) - \sum_{i=1}^{n} t_i(t_i-1)(2t_i+5)}{18} \quad (4)$$

3. Results

3.1 Relationship between cloud cover and aridity index

The study reveals the annual cloud cover are significant correlated to the AI over the MP and surrounding areas from 1979~2019, which can be used for subsequent studies. Cloud clover parameters are characterized by a significant impact. The whole area of aridity conditions presents a significant negative correlation relationship, which means that The AI decrease will decrease as the cloud cover increases. The LCC for the aridity degree is most obvious, with 97.17 % of the area showing a significant negative correlation. In a general way, more cloud cover will increase the precipitation probability and reduce the surface evaporation, which will make the area moist. The surface cover/land use and human activity intensity are different, leading to spatial heterogeneity.

3.2 Spatiotemporal variation characteristics of parameters

1) Cloud cover

Cloud cover has generally been below the mean since 1995. The LCC is more than 15 % below the mean of 1979~2019. The annual mean TCC is 47.38 % and generally been below the average for 16 years after 1999. HCC was 31.64 %, while LCC and MCC were 13.19 % and 26.43 %, respectively. All three types of cloud cover reduced significantly after 1999. The overall cloud cover of the MP and surrounding areas showed a downward trend. Thus, the decrease in cloud cover is the direct cause of the decrease in TP. It also leads to an increase in surface radiation, which in turn leads to an increase in PE.

The annual mean spatial distribution of different cloud cover over the MP and surrounding areas from 1979~2019 is shown in Figure 2. Different cloud covers are higher in the northern region of 50°N and lower in the latitude region of 40°N~45°N. For example, the TCC is >55 % in the northern region of 50°N and <45 % in the latitude region of 40°N~45°N. In the seasonal variation in different cloud covers, the TCC and HCC increase from spring to summer and decrease from autumn to winter in the latitude region of 40°N~45°N. In winter, the HCC reached 70 % in the northwest of the study area. The overall changes in LCC and MCC are small. It is less cloud cover in the Midwest over the MP, more in the east and north, and HCC are more than LCC (Bao et al., 2018). The spatial distribution characteristics of LCC and TCC are similar to the aridity index.

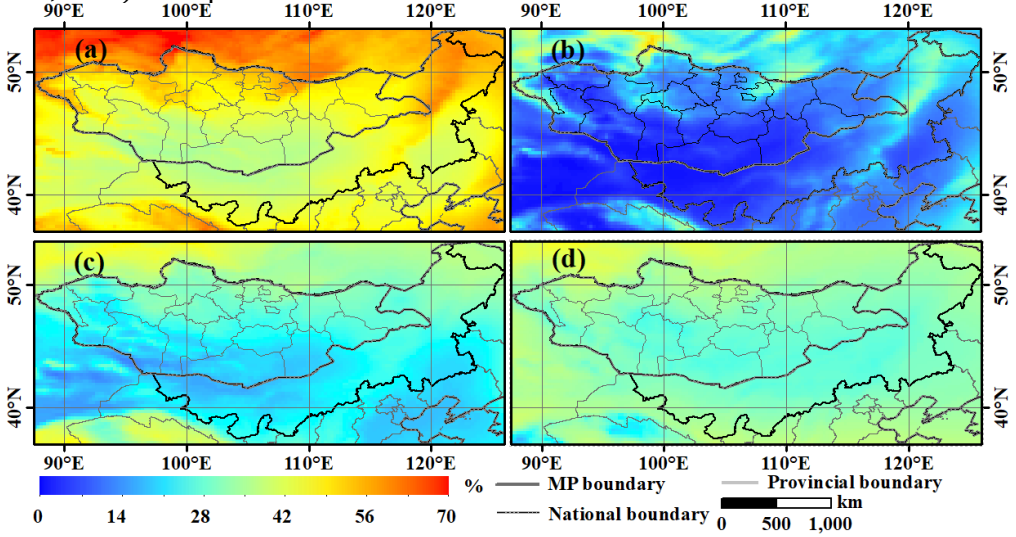

Fig. 2 Spatial distribution of annual cloud cover over the MP and surrounding areas from 1979~2019: (a) Total cloud cover, (b) Low cloud cover, (c) Medium cloud cover, and (d) High cloud cover

2) Aridity index

The spatial and temporal distribution characteristics of the AI were studied which shows the characteristics of age changes. The spatiotemporal variation characteristics and variation trend of annual AI were studied. The AI has been above an average of 40 % for 13 of the 21 years from 1999~2019. The annual mean AI is 5.54, and the perennial aridity condition presents a fluctuating trend from 1979~2019. The degree of aridity years of the change trend shows significant growth at a rate of approximately 0.47 per decade (through the 0.05 level of significance test). It presents a significant trend of aridity.

The spatial distribution annual mean AI of the MP and surrounding areas from 1979~2019 are shown (Figure 3). The variation trend ZS is calculated. According to the AI classification standard, the MP is in the arid and semiarid areas, with a total area of 85.03 %; the arid area is as high as 40.62 %, and the humid areas are mainly located in the northeast region of Inner Mongolia and are scattered across the MP. An analysis of the change trend shows that most areas of the MP show a trend of aridity, accounting for 94.29 % (69.47 % passed the significance test at the level of 0.05). Among them, the trend of aridity in Mongolia is relatively serious compared with Inner Mongolia in China.

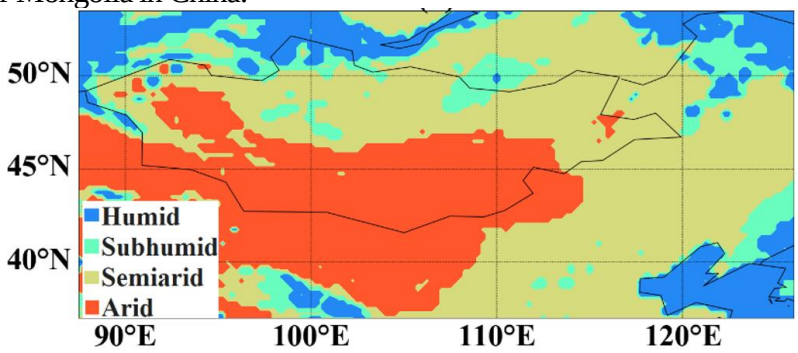

Fig. 3 Spatial distribution of the annual mean aridity index over the MP and surrounding areas from 1979~2019.

3.3 The effect of cloud cover on aridity

Cloud cover can affect precipitation, and cloud cover affect surface radiation, which in turn affects evaporation. As Figure 4 shows we study the annual and monthly regional mean and variation trends of TP and PE over the MP and surrounding areas from 1979~2019 that TP is below the mean of 50 mm after 1999, and the PE is 50 mm above the mean after 1999. TP is the highest in July, with a median of 90 mm, while PE is the highest between May and August, with a median of 140 mm. The annual mean TP is 415.20 mm, and the PE is 891.33 mm for the whole region of the MP and surrounding areas. TP presents a fluctuating downward trend from 1979~2019, with an annual change trend at a rate of approximately 22 mm/decade and a significant decline (based on the 0.05 level of significance test). PE presents a wave rising trend, and the annual variation trend is significant at a rate of approximately 25 mm/decade (based on the 0.05 level of significance test). Therefore, PE is higher than TP, and the gap between the two parameters increases.

The direct cause of the aridity in the central and western regions of the MP is TP less than 340 mm and PE higher than 1000 mm. The 85.20 % area of the TP is <630 mm, while the PE of the corresponding area is 1020~1208 mm. Therefore, except for the southeastern ocean area and the northwest forest area of the study area, the PE is generally higher than the TP. The spatial and temporal variations in TP and PE are similar. There is a general decline in the TP, and PE is generally an upward trend, but there are spatial heterogeneity changes. Particularly at 105°E~126°E, 40~45°N, PE increases and TP declines. However, the TP in some regions of 87.5°E~95°E and 50~53.5°N shows an upward trend, while the PE shows a downward trend. In general, the TP in a large area is much lower than the PE, and the TP continues to decrease, while the PE increases (Yin-Tai et al., 2019; Li et al., 2018; Vetter et al., 2012). The spatial distribution of TP is similar to the AI.

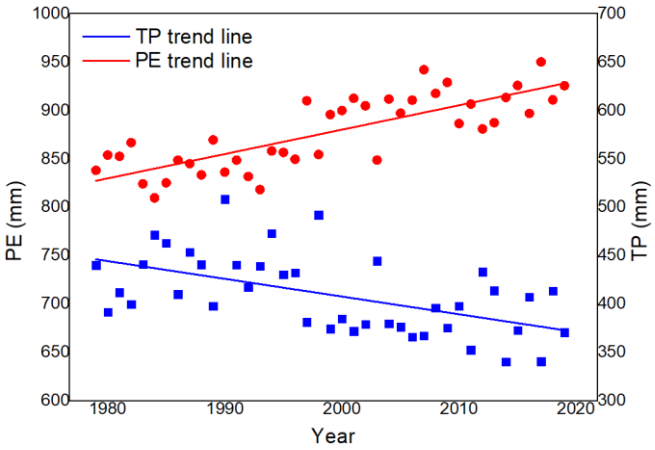

Fig. 4 The annual mean and variation trend of total precipitation and Potential evaporation over the MP and surrounding areas from 1979~2019

We study the anomalous and variation trend of annual mean surface radiation over the MP and surrounding areas from 1979 ~2019 that surface radiation has generally been above average since 1995. The SNSR is 3 % higher, the SNLR is 4 % higher and the R_n is 3 % higher than the mean. For the entire region, the annual mean of R_n is 1805.67 MJ/m^2, the SNSR is 4362.88 MJ/m^2 and the SNLR is 2257.22 MJ/m^2. The two parameters increase at a rate of 2 %/decade (through the 0.05 level of significance test). R_n is 1 % and shows an increasing trend from 1979~2019. An increase in surface radiation will lead to an increase in PE. The increase in surface radiation is mainly related to the reduction in cloud cover, which leads to a reduction in the cloud radiative forcing.

As Figure 5 shows the spatial distribution of annual and seasonal instantaneous values of the R_n, SNSR and SNLR in 1979~2019 over the MP and surrounding areas. In the annual distribution, the R_n in midwest of the MP is <2000 MJ/m^2. The value of SNSR decreased with increasing latitude from 2261~5814 MJ/m^2. The SNLR is higher in the latitude of 40°N~45°N in the range of 1326~3841 MJ/m^2 and lower in other areas. Among the four seasons, summer is the highest radiation season, in which most of the mean SNSR is 1679 MJ/m^2, while the mean SNLR is 713 MJ/m^2. It is close to the existing research results (Chenghai et al., 2011). In particular, the spatial distribution characteristics of SNLR are similar to the AI.

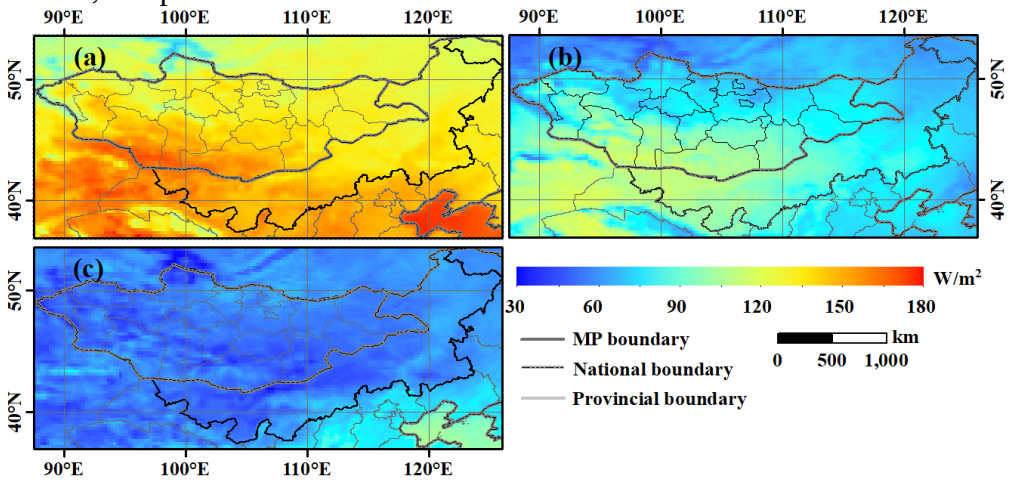

Fig. 5 Spatial distribution of annual values from 1979~2019 over the MP and surrounding areas: (a) Surface total radiation, (b) Surface net shortwave radiation, and (c) Surface net longwave radiation

4. Conclusion and discussion

This study reveals the cloud cover parameters are significantly negatively correlated with the AI. Spatiotemporal variation characteristics of the aridity are the central and western regions of the study area are arid and semi-arid, and worst in spring and keep increased from 1979~2019. In particular, aridity intensified after 1999. Spatiotemporal variation characteristics of the cloud cover are similar to the AI. Less cloud cover leads to less TP and more PE, and PE keep increases while TP decreases. The cloud cover is low and continues

to decrease. In particular, the cloud cover is less in the central and western regions results in reduced TP and increased surface radiation. The higher surface radiation caused the PE to rise.

This paper studies the influence of energy and water cycle parameters on aridity, and the conclusion is helpful for disaster prevention and mitigation over the MP and surrounding areas. However, we did not combine the energy and water cycle, atmospheric circulation, vegetation cover and other comprehensive factors to study the aridity over the MP and surrounding areas, so this combination will be addressed in our future research work.

Acknowledgments

This article has not been published. The authors are very grateful to European Centre for Medium Range Weather Forecasting (ECMWF) ERA5 for making the data available and providing elaborate documentation of the algorithms. The ERA5 data provided by Climate Data Store, are available from https://cds.climate.copernicus.eu/.

References

Allan, R. 2011. Combining satellite data and models to estimate cloud radiative effect at the surface and in the atmosphere. Meteorological Applications, 18, 324-333. https://doi.org/10.1002/met.285.

Alley, W. M. 1984. The palmer drought severity index - limitations and assumptions. Journal of Climate and Applied Meteorology, 23, 1100-1109. https://doi.org/10.1175/1520-0450(1984)023 %3C1100:TPDSIL %3E2.0.CO;2.

Balsamo, G.,Albergel, C.,Beljaars, A.,Boussetta, S. and Vitart, F. 2015. ERA-Interim/Land: A global land surface reanalysis dataset. Hydrology & Earth System Sciences, 19, 389-407. https://doi.org/10.5194/hess-19-389-2015.

Bao, S.,Letu, H.,Zhao, J.,Lei, Y.,Zhao, C.,Li, J.,Tana, G.,Liu, C.,Guo, E. and Zhang, J. 2020. Spatiotemporal distributions of cloud radiative forcing and response to cloud parameters over the Mongolian Plateau during 2003–2017. International Journal of Climatology, 40. https://doi.org/10.1002/joc.6444.

Bao, S.,Letu, H.,Zhao, C.,Tana, G.,Shang, H.,Wang, T.,Lige, B.,Bao, Y.,Purevjav, G. and He, J. 2018. Spatiotemporal Distributions of Cloud Parameters and the Temperature Response Over the Mongolian Plateau During 2006–2015 Based on MODIS Data. IEEE Journal of Selected Topics in Applied Earth Observations and Remote Sensing, 12, 1-10. https://doi.org/10.1109/JSTARS.2018.2857827.

Bauer, P.,Lopez, P.,Moreau, E.,Chevallier, F. and Bonazzola, M. 2007. The European Centre for Medium-Range Weather Forecasts Global Rainfall Data Assimilation Experimentation, Springer Netherlands. https://doi.org/10.1007/978-1-4020-5835-6_35.

Bengtsson, L.,Hagemann, S. and Hodges, K. I. 2004. Can climate trends be calculated from reanalysis data? Journal of Geophysical Research, 109. https://doi.org/10.1029/2004JD004536.

Betts, A. K.,Hong, S. Y. and Pan, H. L. 1996. Comparison of NCEP-NCAR Reanalysis with 1987 FIFE Data. Monthly Weather Review, 124, 1480-1498. https://doi.org/10.1175/1520-0493(1996)124 %3C1480:CONNRW %3E2.0.CO;2.

Breiman, L. 2001. Random Forests. Machine Learning, 45, 5-32. https://doi.org/10.1023/A:1010933404324.

Bremer, D.,Auen, L.,Ham, J. and Owensby, C. 2001. Evapotranspiration in a Prairie Ecosystem: effects of Grazing by Cattle. Agronomy Journal, 93. https://doi.org/10.2134/agronj2001.932338x.

Cao, X.,Feng, Y. and Wang, J. 2017. Remote sensing monitoring the spatio-temporal changes of aridification in the Mongolian Plateau based on the general Ts-NDVI space, 1981–2012. Journal of Earth System Science, 126. https://doi.org/10.1007/s12040-017-0835-x.

Chenghai, Wang, and, Zhifu, Zhang, and, Wenshou and Tian 2011. Factors affecting the surface radiation trends over China between 1960 and 2000. Atmospheric Environment.

https://doi.org/10.1016/j.atmosenv.2011.02.028.

Dyn, C.,Bao, G.,Liu, Y.,Liu, N. and Linderholm, H. 2014. Drought variability in eastern Mongolian Plateau and its linkages to the large-scale climate forcing. Climate Dynamics, 44. https://doi.org/10.1007/s00382-014-2273-7.

Gao, T.,Si, Y.,Yu, X.,Wulan,Yang, P. and Gao, J. 2019. A seasonal forecast scheme for the Inner Mongolia spring drought: Part-I: dynamic characteristics of the atmospheric circulation and forecast signals. Theoretical and applied climatology, 135, 519-532. https://doi.org/10.1007/s00704-018-2403-y.

Hessl, A. E.,Anchukaitis, K. J.,Jelsema, C.,Cook, B.,Byambasuren, O.,Leland, C.,Nachin, B.,Pederson, N.,Tian, H. and Hayles, L. A. 2018. Past and future drought in Mongolia. Adv, 4, e1701832. https://doi.org/10.1126/sciadv.1701832.

Hong, H.,Xiaoling, G. and Hua, Y. Variable selection using Mean Decrease Accuracy and Mean Decrease Gini based on Random Forest. 2016 7th IEEE International Conference on Software Engineering and Service Science (ICSESS), 26-28 Aug. 2016. 219-224. https://doi.org/10.1109/ICSESS.2016.7883053.

Hu, Y.,Wen, J.,Ma, Y.,Huang, Y. and Xu, J. 2018. Research on the Relationship Between the Spatial and Temporal Variation of Greenup and Precipitation in Mongolian Plateau, international conference on agro geoinformatics, 1-5. https://doi.org/10.1109/agro-geoinformatics.2018.8476130.

Jin,Zhang,Wang,Bao and Guo 2019. Analysis for Spatio-Temporal Variation Characteristics of Droughts in Different Climatic Regions of the Mongolian Plateau Based on SPEI. Sustainability, 11, 5767. https://doi.org/10.3390/su11205767

Katata, G.,Nagai, H.,Wrzesinsky, T.,Kle mm, O.,Eugster, W. and Burkard, R. 2008. Development of a Land Surface Model Including Cloud Water Deposition on Vegetation. Journal of Applied Meteorology and Climatology, 47, 2129-2146. https://doi.org/10.1175/2008JAMC1758.1.

Kendall, M. G. 1990. Rank correlation methods. 25, 86–91. https://doi.org/10.1111/j.2044-8295.1934.tb00727.x.

Li, C., Filho, W., Yin, J., Hu, R., Wang, J., Yang, C., Yin, S., Bao, Y. and Ayal, D. 2018. Assessing vegetation response to multi-time-scale drought across inner Mongolia plateau. Journal of Cleaner Production, 179, 210-216. https://doi.org/10.1016/j.jclepro.2018.01.113

Li, W.,Duan, L.,Luo, Y.,Liu, T. and Scharaw, B. 2018. Spatiotemporal Characteristics of Extreme Precipitation Regimes in the Eastern Inland River Basin of Inner Mongolian Plateau, China. Water, 10, 35. https://doi.org/10.3390/w10010035.

Mann, H. B. 1945. Non-Parametric Test Against Trend. Econometrica, 13, 245-259. https://doi.org/10.2307/1907187.

McKee, T.,Doesken, N. and Kleist, J. 1993. The Relationship of Drought Frequency and Duration to Time Scales. paper presented at 8th Conference on Applied Climatology, Am. Meteorol. Soc., Anaheim, Calif., 17.

Molod, A.,Vikhliaev, Y. V.,Hackert, E. C.,Kovach, R. M.,Zhao, B.,Cullather, R. I.,Marshak, J.,Borovikov, A.,Li, Z. and Barahona, D. GEOS S2S-2_1: The GMAO new high resolution Seasonal Prediction System. Agu Fall Meeting, 2017. https://doi.org/10.1029/2019JD031767.

Pedram, S.,Wang, X.,Liu, T. and Duan, L. 2017. Simulated dynamics of soil water and pore vapor in a semiarid sandy ecosystem. Journal of Arid Environments, 151. https://doi.org/10.1016/j.jaridenv.2017.11.004.

Penman, H. 1948. Natural Evaporation From Open Water, Bare Soil and Grass. Proceedings of The Royal Society A: Mathematical, Physical and Engineering Sciences, 193, 120-145. https://doi.org/10.1098/rspa.1948.0037.

Qian, Y.,Kaiser, D. P.,Leung, L. R. and Xu, M. 2015. More frequent cloud-free sky and less surface solar radiation in China from 1955 to 2000. Geophysical Research Letters, 33. https://doi.org/10.1029/2005GL024586.

Song, X.,Leng, P.,Li, Z.-L.,Tang, B.,Li, X.,Ma, J. and Zhou, F. 2012. Soil moisture

estimation using a slope indicator between land surface temperature and net surface shortwave radiation, Egu General Assembly Conference EGU General Assembly Conference Abstracts, 3814.

Tong, S.,Lai, Q.,Zhang, J.,Bao, Y. and Zhang, F. 2018. Spatiotemporal drought variability on the Mongolian Plateau from 1980–2014 based on the SPEI-PM, intensity analysis and Hurst exponent. Science of The Total Environment, 615. https://doi.org/10.1016/j.scitotenv.2017.09.121

Torres-Alavez, J. 2018. Quantifying the Relative Roles of Land Use Change and Remote Forcing on the 1930s Dust Bowl Drought, Dissertation Abstracts International, 79-09, 120.

Urraca, R.,Huld, T.,Gracia-Amillo, A.,Kaspar, F. and Sanz-Garcia, A. 2018. Evaluation of global horizontal irradiance estimates from ERA5 and COSMO-REA6 reanalyses using ground and satellite-based data, Solar Energy, 164, 339-354. https://doi.org/10.1016/j.solener.2018.02.059.

Vetter, S. H., Schaffrath, D. and Bernhofer, C. 2012. Spatial simulation of evapotranspiration of semi-arid Inner Mongolian grassland based on MODIS and eddy covariance data. Environmental Earth ences, 65, 1567-1574. https://doi.org/10.1007/s12665-011-1187-5

Vicente-Serrano, S.,Beguería, S. and López-Moreno, J. I. 2010. A Multiscalar Drought Index Sensitive to Global Warming: The Standardized Precipitation Evapotranspiration Index. Journal of Climate, 23, 1696-1718. https://doi.org/10.1175/2009JCLI2909.1.

Weerts, A.,Winsemius, H.,Dutra, E.,Beckers, J.,Brolsma, R. J.,Van Beek, L. P. H.,Pappenberger, F.,Westerhoff, R. and Bierkens, M. F. P. 2013. Seasonal Predictability of Water Scarcity at the Global Scale, Geophysical Research Abstracts, 15.

Wu, S.,Yin, Y.,Zheng, D. and Yang, Q. 2006. Moisture conditions and climate trends in China during the period 1971–2000. International Journal of Climatology, 26, 193-206. https://doi.org/10.1002/joc.1245.

Wu, W. and Wang, S. G. 2011. Tendency change of cloud cover over northern China and its relation with regional climate. Plateau Meteorology, 30, 651-658. https://doi.org/10.3724/SP.J.1146.2006.01085

Yao, Y.,Liang, S.,Qin, Q.,Wang, K. and Zhao, S. 2011. Monitoring global land surface drought based on a hybrid evapotranspiration model. Internatonal Journal of Applied Earth Observation and Geoinformation, 13, 447-457. https://doi.org/10.1016/j.jag.2010.09.009.

Yin-Tai, N. A.,Fu-Ying, Q.,Gen-Suo, J.,Jie, Y. and Yu-Hai, B. 2019. Change trend and regional differentiation of precipitation over the Mongolian Plateau in recent 54 years. Arid Land Geography, 42, 1253-1261. https://doi.org/10.12118/j.issn.1000-6060.2019.06.03

Young, D. T.,Perraut, S.,Roux, A.,Villedary, C. D.,Gendrin, R.,Korth, A.,Kremser, G. and Jones, D. 2012. Wave-particle interactions near Ω He +Observed on GEOS 1 and 2, 1. Propagation of ion cyclotron waves in He +-rich plasma. Journal of Geophysical Research Space Physics, 86, 6755-6772. https://doi.org/10.1029/JA086iA08p06755.